University of New Orleans
ScholarWorks@UNO

Electrical Engineering Faculty Publications | Department of Electrical Engineering

9-1-2010

Return-path, multiple-principal-angle, internal-reflection ellipsometer for measuring IR optical properties of aqueous solutions

Rasheed M.A. Azzam
University of New Orleans, razzam@uno.edu

Follow this and additional works at: https://scholarworks.uno.edu/ee_facpubs

Part of the Bioimaging and Biomedical Optics Commons, and the Electrical and Electronics Commons

Recommended Citation
R. M. A. Azzam, "Return-path, multiple-principal-angle, internal-reflection ellipsometer for measuring IR optical properties of aqueous solutions," Appl. Opt. 49, 4710-4714 (2010) http://www.opticsinfobase.org/ao/abstract.cfm?URI=ao-49-25-4710

This Article is brought to you for free and open access by the Department of Electrical Engineering at ScholarWorks@UNO. It has been accepted for inclusion in Electrical Engineering Faculty Publications by an authorized administrator of ScholarWorks@UNO. For more information, please contact scholarworks@uno.edu.

Return-path, multiple-principal-angle, internal-reflection ellipsometer for measuring IR optical properties of aqueous solutions

R. M. A. Azzam

Department of Electrical Engineering, University of New Orleans, New Orleans, Louisiana 70148, USA (razzam@uno.edu)

Received 18 June 2010; accepted 26 July 2010;
posted 4 August 2010 (Doc. ID 130335); published 24 August 2010

A retroreflection (return-path) spectroscopic ellipsometer without a wave plate is described that uses an IR-transparent high-refractive-index hemicylindrical semiconductor substrate to measure the optical properties of aqueous solutions from multiple principal angles and multiple principal azimuths of attenuated internal reflection (AIR) at the semiconductor–solution interface. The pseudo-Brewster angle of minimum reflectance for the p polarization is also readily measured using the same instrument. This wealth of data can also be used to characterize thin films at the solid–liquid interface. Simulated results of AIR at the Si–water interface over the 1.2–11 μm IR spectral range are presented in support of this concept. The optical properties of water and aqueous solutions are important for modeling radiative transfer in the atmosphere and oceans and for biomedical and tissue optics. © 2010 Optical Society of America

OCIS codes: 120.2130, 160.4760, 240.0240, 260.5430.

1. Introduction

Ellipsometry is an important technique for surface and thin film analysis that is based on measurement of the change of the state of polarization of light upon reflection with broad application in science and technology. It is, therefore, not surprising that numerous ellipsometers of different designs have been proposed and implemented [1–5].

Ellipsometry at the principal angle of incidence, at which the differential reflection phase shift $\Delta = \pm\pi/2$, is attractive because of the high precision associated with the detection of this condition [6–9] and because a simple instrument that employs the return-path (autocollimation or retroreflection) configuration [10–17] can be used.

In this paper, a novel multiple-principal-angle return-path ellipsometer (MPA RPE) is described that is particularly suited for measurement of the IR optical properties of water and aqueous solutions using internal reflection at a semiconductor (Si)–liquid interface. Most of the reported optical properties of water and aqueous solutions are determined using reflectance, refraction, and transmittance measurements [18–24], but not ellipsometry. Optical constants (n and k) of water and aqueous solutions are of great interest in radiative transfer in the ocean and atmosphere and also in biomedical applications and tissue optics. Few articles that deal with internal-reflection ellipsometry at solid–liquid interfaces have been published recently [25–27].

In Section 2, the MPA RPE is described. In Section 3, a published dispersion relation [28] for Si (which is IR transparent) and the tabulated optical constants of water of Hale and Querry [20] are used to calculate the multiple principal angles and associated principal azimuths $(\bar{\phi}_i, \bar{\psi}_i)$, $i = 1, 2, 3$ of the Si–water interface over the 1.2–11 μm IR wavelength range. Over much of this spectral range,

0003-6935/10/254710-05$15.00/0
© 2010 Optical Society of America

the fractional complex relative dielectric function $\varepsilon = \varepsilon_w/\varepsilon_{\rm Si}$ of the Si–water interface falls inside the domain of MPA of the complex plane [29,30]. In Section 4 the pseudo-Brewster angle $\phi_{\rm pB}(\lambda)$ of minimum reflectance for the p polarization [31] of the Si–water interface, which is readily measurable using the same RPE, is also determined as a function of wavelength λ. The wealth of data that the MPA RPE provides can be used (in reverse) to determine the optical constants of water and aqueous solutions and also to characterize thin interfacial layers at the Si–water interface. Section 5 provides a brief summary of this work.

2. Multiple-Principal-Angle Return-Path Ellipsometer

Figure 1 shows the optical setup of the MPA RPE. Collimated monochromatic light from source L passes through beam splitter BS and linear polarizer P that can be rotated around the light beam as an axis. Linearly polarized light transmitted by P is internally reflected at center O of the planar face AB of a polished hemicylindrical semiconductor (Si) substrate or sample S at an angle of incidence ϕ measured from the surface normal ON. The aqueous solution is contained in the rectangular space (cuvette) ABCD. The thickness of the liquid cell of a few millimeters is $\gg$ the penetration depth of IR light into the aqueous solution. The surface of the entrance quadrant AN of the hemicylinder has a broadband antireflection coating (ARC), whereas the remaining quadrant BN is uncoated (UC). The reflected beam in the radial direction OR is retroreflected at normal incidence by the Si–air interface at R, experiences a second reflection at O, is transmitted by polarizer P, and is reflected off BS to photodetector D. Sample S is mounted on a goniometer (not shown) that can be rotated around the cylinder axis at O, which is normal to the plane of the page in Fig. 1. (The polarizer transmission-axis azimuth P, measured from the plane of incidence, and angle of incidence ϕ can be determined with a precision of 0.001° using commercially available rotational mounts [17]). As in O'Bryan's original vacuum ellipsometer [10], the polarizer and sample are rotated until the output electrical signal of detector D is extinguished. Under this null condition, the reflected beam OR is circularly polarized, the incidence angle is the principal angle, $\phi = \bar{\phi}$, and the polarizer azimuth equals the principal azimuth, $P = \pm\bar{\psi}$.

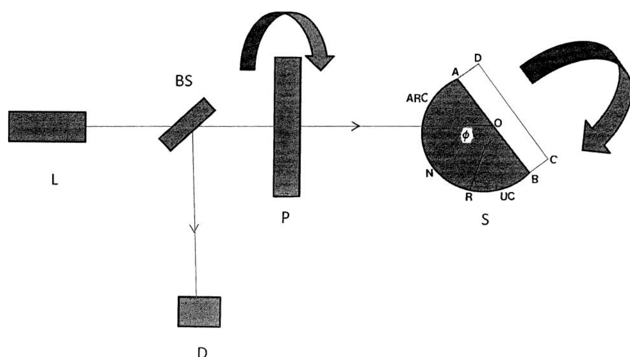

Fig. 1. Multiple-principal-angle return-path ellipsometer (MPA RPE) that consists of a source of collimated monochromatic light L, beam splitter BS, and linear polarizer P that can be rotated around the light beam as an axis. Sample S is a polished hemicylindrical semiconductor (Si) substrate that allows internal reflection at a variable angle of incidence ϕ measured from the surface normal ON. An aqueous solution is contained in the rectangular space (cuvette) ABCD. The surface of the entrance quadrant AN of the hemicylinder has a broadband antireflection coating (ARC), whereas the remaining quadrant BN is uncoated (UC). Arrows indicate the forward and backward propagation directions.

3. Multiple Principal Angles and Multiple Principal Azimuths of the Si–Water Interface

The refractive index of IR-transparent Si is calculated from a dispersion relation given by Tropf *et al.* [28]. The real and imaginary parts n_w and k_w, respectively, of the complex refractive index of water as functions of wavelength are obtained from the tabular data of Hale and Querry [20]. Internal reflection at the Si–water interface is determined by the complex relative dielectric function

$$\varepsilon = \varepsilon_w/\varepsilon_{\rm Si} = \varepsilon_r - j\varepsilon_i, \qquad \varepsilon_r = (n_w^2 - k_w^2)/n_{\rm Si}^2,$$
$$\varepsilon_i = 2n_w k_w/n_{\rm Si}^2. \tag{1}$$

Figure 2 shows ε_r, ε_i of the Si–water interface plotted versus wavelength λ in the 1.2–11 μm spectral range. Figure 3 presents the trajectory of ε_r, ε_i in the complex ε plane as λ is increased from 1.2 to 11 μm. The highlighted domain of MPA shown

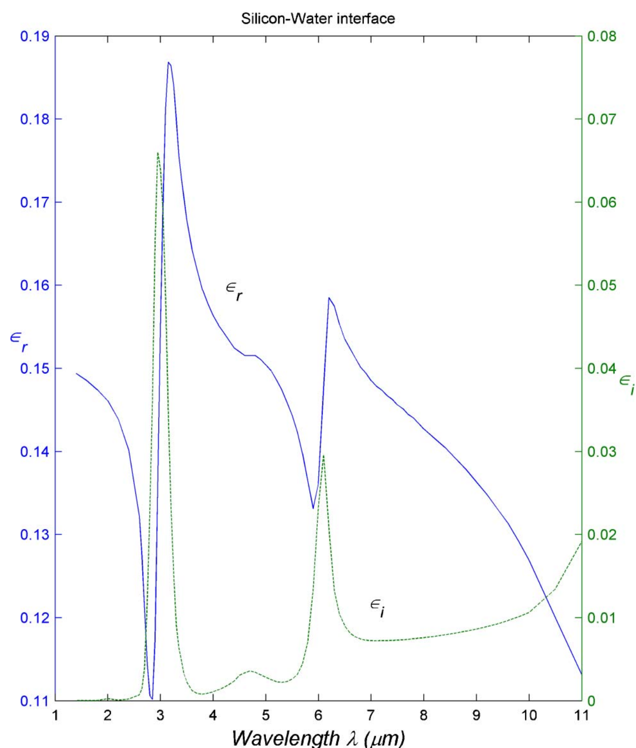

Fig. 2. (Color online) Real and imaginary parts ε_r, ε_i of the relative complex dielectric function of the Si–water interface plotted versus wavelength λ in the 1.2–11 μm spectral range.

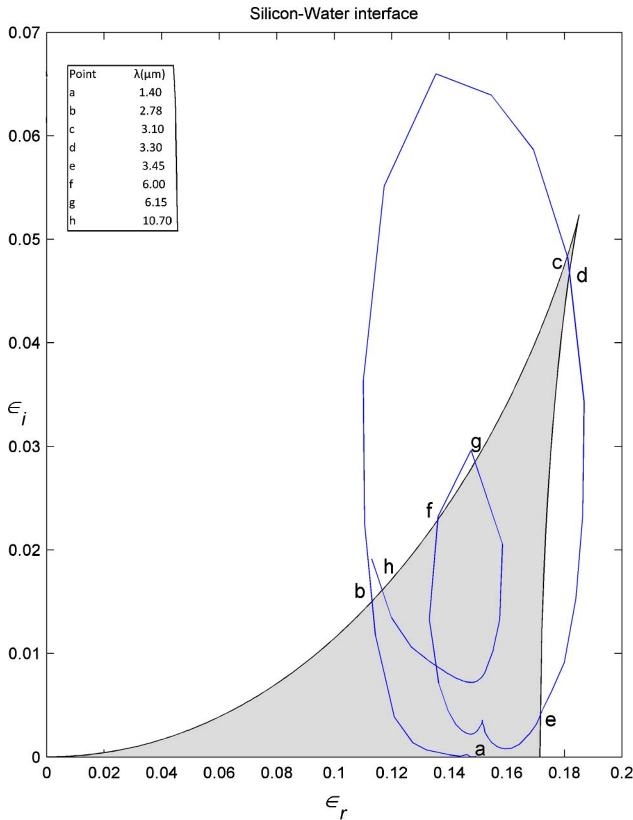

Fig. 3. (Color online) Trajectory of ε_r, ε_i of the Si–water interface in the complex ε plane as the wavelength λ is increased from 1.2 to 11 μm. The domain of multiple principal angles (MPA) is highlighted. The inset gives the wavelengths at points $a, b, c, \ldots,$ and h at which the segmented locus of ε_r, ε_i cuts in and out of the domain of MPA.

in Fig. 3 is determined exactly as described in [29,30]. The inset in Fig. 3 gives the wavelengths at points $a, b, c, \ldots,$ and h at which the segmented locus of ε_r, ε_i cuts in and out of the domain of MPA.

For a given complex ε, up to three principal angles $\bar{\phi}_i$, $i = 1, 2, 3$ are obtained by finding all the acceptable roots of the cubic equation [29,30]:

$$a_3u^3 + a_2u^2 + a_1u + a_0 = 0, \tag{2}$$

$$a_0 = \varepsilon_r^2 + \varepsilon_i^2, \qquad a_1 = -2(a_0 + \varepsilon_r),$$
$$a_2 = a_0 + 4\varepsilon_r + 1, \qquad a_3 = -2(\varepsilon_r + 1), \tag{3}$$

$$u = \sin^2 \bar{\phi}_i. \tag{4}$$

At each principal angle $\bar{\phi}$, the associated principal azimuth $\bar{\psi}$ is calculated from the ratio of complex reflection coefficients for the p and s polarizations, which is purely imaginary:

$$\bar{\rho} = r_p/r_s = \frac{\sin\bar{\phi}\tan\bar{\phi} - (\varepsilon - \sin^2\bar{\phi})^{1/2}}{\sin\bar{\phi}\tan\bar{\phi} + (\varepsilon - \sin^2\bar{\phi})^{1/2}} = j\tan\bar{\psi}. \tag{5}$$

Figure 4 shows the first principal angle and first principal azimuth $\bar{\phi}_1$, $\bar{\psi}_1$ (in degrees) of the Si–water interface plotted versus λ in the 1.2 to 11 μm wavelength range. Salient spectral features of $\bar{\phi}_1$, $\bar{\psi}_1$ in Fig. 4 appear near 3 and 6 μm and correspond to similar features of ε_r, ε_i near the same wavelengths in Fig. 2.

The second and third sets of principal angles and principal azimuths $\bar{\phi}_2$, $\bar{\psi}_2$ and $\bar{\phi}_3$, $\bar{\psi}_3$ (in degrees) of the Si–water interface are plotted in Figs. 5 and 6, respectively, as functions of wavelength λ in the 1.2 to 11 μm spectral range. The second and third solutions cease to exist (as represented by gaps in Figs. 5 and 6) in wavelength ranges in which the trajectory of ε_r, ε_i is outside the domain of MPA in Fig. 3.

The simulated results shown in Figs. 4–6 represent extensive data available from the MPA RPE and that can be used to determine the bulk IR optical properties of an aqueous solution and characterize thin transition layers at the solid–liquid interface. Each principal-angle—principal-azimuth pair $\bar{\phi}_i$, $\bar{\psi}_i$ provides an independent determination of the real and imaginary parts of the complex dielectric function of water (or aqueous solution) at each measurement wavelength [29]:

$$\varepsilon_{rw} = \varepsilon_{\mathrm{Si}}(\sin^2\bar{\phi}_i + \sin^2\bar{\phi}_i\tan^2\bar{\phi}_i\cos 4\bar{\psi}_i),$$
$$\varepsilon_{iw} = \varepsilon_{\mathrm{Si}}(\sin^2\bar{\phi}_i\tan^2\bar{\phi}_i\sin 4\bar{\psi}_i). \tag{6}$$

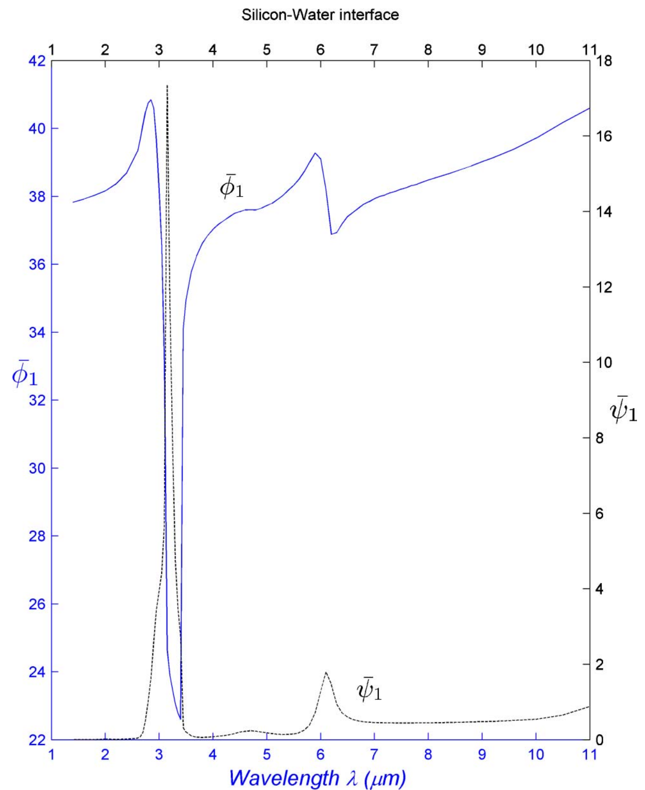

Fig. 4. (Color online) First principal angle and first principal azimuth $\bar{\phi}_1$, $\bar{\psi}_1$ (in degrees) of the Si–water interface plotted versus wavelength λ in the 1.2–11 μm spectral range.

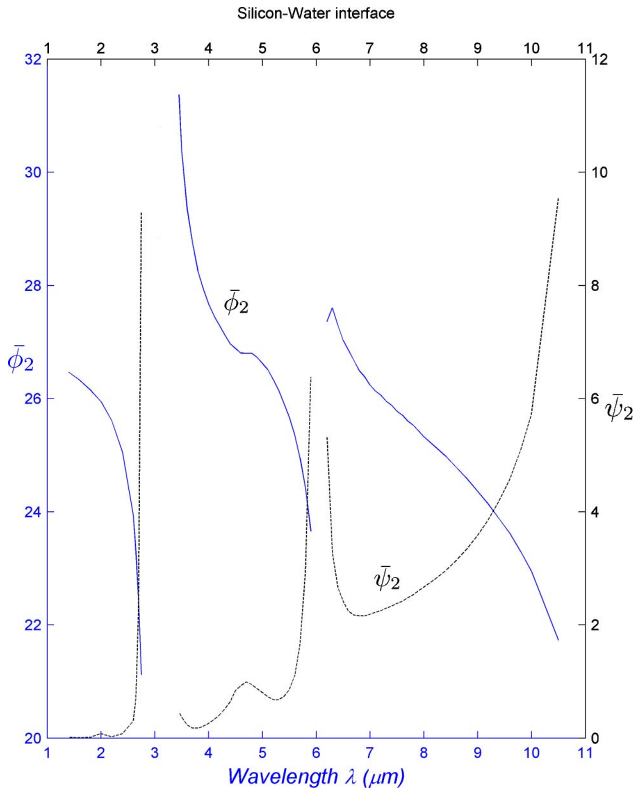

Fig. 5. (Color online) Second principal angle and second principal azimuth $\bar{\phi}_2, \bar{\psi}_2$ (in degrees) of the Si–water interface plotted versus wavelength λ in the 1.2–11 μm spectral range.

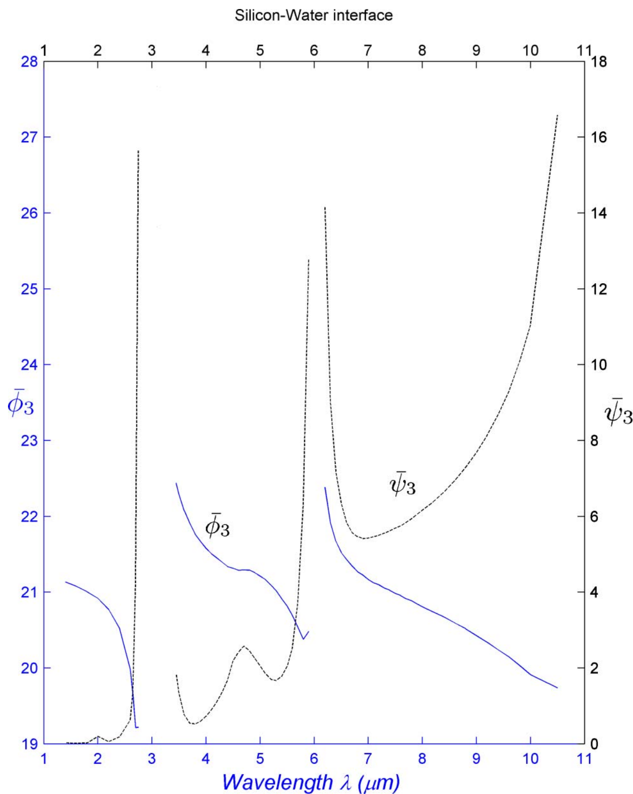

Fig. 6. (Color online) Third principal angle and third principal azimuth $\bar{\phi}_3, \bar{\psi}_3$ (in degrees) of the Si–water interface plotted versus wavelength λ in the 1.2–11 μm spectral range.

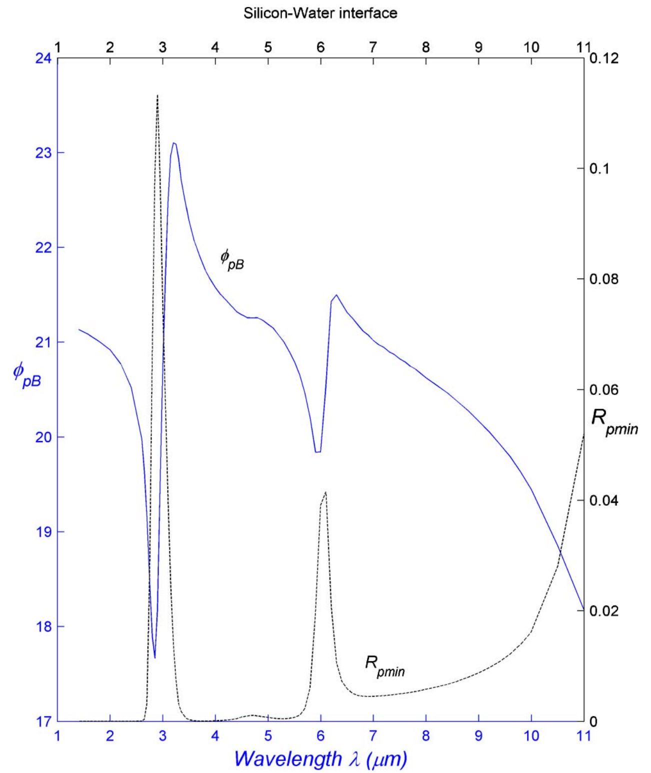

Fig. 7. (Color online) Pseudo-Brewster angle $\phi_{\rm pB}$ (in degrees) and the associated minimum parallel reflectance $R_{p\,\rm min}$ of the Si–water interface plotted as functions of wavelength λ in the 1.2–11 μm spectral range.

4. Pseudo-Brewster Angle of Minimum Parallel Reflectance

If the transmission axis of polarizer P in Fig. 1 is oriented parallel (p) to the plane of incidence and sample S is rotated so that the return signal (output of detector D) is minimized, the pseudo-Brewster angle $\phi_{\rm pB}$ of the Si–liquid interface can be measured.

The pseudo-Brewster angle $\phi_{\rm pB}$ of the Si–water interface is calculated from the complex ε data shown in Fig. 2 by solving a different cubic equation [31]:

$$a_3u^3 + a_2u^2 + a_1u + a_0 = 0, \tag{7}$$

$$a_0 = (\varepsilon_r^2 + \varepsilon_i^2)^2, \qquad a_1 = -2a_0,$$
$$a_2 = a_0 - 3\sqrt{a_0}, \qquad a_3 = 2\varepsilon_r + 2\sqrt{a_0}, \tag{8}$$

$$u = \sin^2 \phi_{\rm pB}. \tag{9}$$

Figure 7 shows $\phi_{\rm pB}$ and, for completeness, the associated minimum parallel reflectance $R_{p\,\rm min}$ as functions of λ for the Si–water interface. The spectrum of $\phi_{\rm pB}(\lambda)$ provides additional information that can be used for consistency checks or overdetermination of the optical properties of the aqueous solution and transition layer obtained from multiple principal-angle—principal-azimuth data.

5. Summary

A novel MPA RP ellipsometer (Fig. 1) is described that is particularly suited for determining the IR optical properties of aqueous solutions using attenuated internal reflection at a Si–liquid interface. These optical properties are important for modeling radiative transfer in the ocean and atmosphere and for biomedical and tissue optics. Furthermore, the extensive data that this relatively simple instrument provides enable the characterization of thin films at solid–liquid interfaces. The high precision associated with PA ellipsometry represents another distinct advantage.

Although results for the Si–water interface are presented here, similar results are obtained if Ge or another high-index IR-transparent semiconductor substrate is used instead of Si. Reference measurements obtained using the MPA RPE of Fig. 1 on an empty cell (i.e., at the Si–air or Ge–air interface) provide independent data that can be used to determine the refractive index of the substrate as a function of wavelength without recourse to published dispersion formulas. It should be noted, however, that residual stress birefringence in the transparent substrate must be negligible; otherwise, such birefringence represents a source of error that has to be accounted for.

The author thanks Irfan Ali for his assistance in performing calculations and generating figures presented in this paper. This work was recently presented at a poster session of the 5th International Conference on Spectroscopic Ellipsometry (ICSE-V), Albany, New York, 23–28 May 2010.

References

1. R. M. A. Azzam and N. M. Bashara, *Ellipsometry and Polarized Light* (North-Holland, 1987).
2. R. Röseler, *Infrared Spectroscopic Ellipsometry* (Akademie-Verlag, 1990).
3. R. M. A. Azzam, ed., *Selected Papers on Ellipsometry*, Vol. MS27 of SPIE Milestone Series (SPIE, 1991).
4. H. G. Tompkins and E. A. Irene, eds., *Handbook of Ellipsometry* (William Andrew, 2005).
5. R. M. A. Azzam, "Ellipsometry," in *Handbook of Optics*, M. Bass and V. N. Mahajan, eds. (McGraw-Hill, 2010), Vol. I.
6. D. E. Aspnes, "Optimizing precision of rotating-analyzer ellipsometers," J. Opt. Soc. Am. **64**, 639–646 (1974).
7. R. M. A. Azzam and A.-R. Zaghloul, "Principal angle, principal azimuth, and principal-angle ellipsometry of film-substrate systems," J. Opt. Soc. Am. **67**, 1058–1065 (1977).
8. D. Chandler-Horowitz and G. A. Candela, "Principal angle spectroscopic ellipsometry utilizing a rotating analyzer," Appl. Opt. **21**, 2972–2977 (1982).
9. L. Schrottke and G. Jungk, "Automated null ellipsometer with rotating analyzer," Rev. Sci. Instrum. **65**, 3657–3660 (1994).
10. H. M. O'Bryan, "The optical constants of several metals in vacuum," J. Opt. Soc. Am. **26**, 122–127 (1936).
11. M. Yamamoto, "New type of precision ellipsometer without employing a compensator," Opt. Commun. **10**, 200–202 (1974).
12. T. Yamaguchi and H. Takahashi, "Autocollimation-type ellipsometer for monitoring film growth through a single window," Appl. Opt. **15**, 677–680 (1976).
13. R. M. A. Azzam, "Oblique and normal-incidence photometric return-path ellipsometer for isotropic and anisotropic surfaces," J. Opt. **9**, 131–134 (1978).
14. M. Yamamoto and O. S. Heavens, "A vacuum automatic ellipsometer for principal angle of incidence measurement," Surf. Sci. **96**, 202–216 (1980).
15. R. M. A. Azzam, "Measurement of the Jones matrix of an optical system by return-path null ellipsometry," J. Mod. Opt. **28**, 795–800 (1981).
16. A. B. Marchant and J. J. Wrobel, "Simple ellipsometer design," Appl. Opt. **20**, 2040–2041 (1981).
17. L. R. Watkins and S. S. Shamailov, "Variable angle of incidence spectroscopic autocollimating ellipsometer," Appl. Opt. **49**, 3231–3234 (2010).
18. M. R. Querry, B. Curnutte, and D. Williams, "Refractive index of water in the infrared," J. Opt. Soc. Am. **59**, 1299–1305 (1969).
19. M. R. Querry, R. C. Waring, W. E. Holland, G. M. Hale, and W. Nijm, "Optical constants in the infrared for aqueous solutions of NaCl," J. Opt. Soc. Am. **62**, 849–855 (1972).
20. G. M. Hale and M. R. Querry, "Optical constants of water in the 200 nm to 200 μm wavelength region," Appl. Opt. **12**, 555–563 (1973).
21. K. F. Palmer and D. Williams, "Optical properties of water in the near infrared," J. Opt. Soc. Am. **64**, 1107–1110 (1974).
22. M. N. Afsar and J. B. Hasted, "Measurements of the optical constants of liquid H_2O and D_2O between 6 and 450 cm^{-1}," J. Opt. Soc. Am. **67**, 902–904 (1977).
23. D. M. Wieliczka, S. Weng, and M. R. Querry, "Wedge shaped cell for highly absorbing liquids: infrared optical constants of water," Appl. Opt. **28**, 1714–1719 (1989).
24. M. Daimon and A. Masumura, "Measurement of the refractive index of distilled water from the near-infrared to the ultraviolet region," Appl. Opt. **46**, 3811–3820 (2007).
25. S. Rekveld, *Ellipsometric Studies of Protein Adsorption onto Hard Surfaces in a Flow Cell* (Fedobruk, 1997).
26. H. Arwin, M. Poksinski, and K. Johansen, "Total internal reflection ellipsometry: principles and applications," Appl. Opt. **43**, 3028–3036 (2004).
27. Y. Mikhaylova, L. Ionov, J. Rappich, M. Gensch, N. Esser, S. Minko, K.-J. Eichhorn, M. Stamm, and K. Hinrichs, "*In-situ* infrared ellipsometric study of stimuli-responsive polyelectrolyte brushes," Anal. Chem. **79**, 7676–7682 (2007).
28. W. J. Tropf, M. E. Thomas, and T. J. Harris, "Properties of crystals and glasses," in *Handbook of Optics*, M. Bass, E. W. Van Stryland, D. R. Williams, and W. L. Wolfe, eds. (McGraw-Hill, 1995), Vol. II, Chap. 33.
29. R. M. A. Azzam, "Contours of constant principal angle and constant principal azimuth in the complex ε plane," J. Opt. Soc. Am. **71**, 1523–1528 (1981).
30. R. M. A. Azzam and A. Alsamman, "Plurality of principal angles for a given pseudo-Brewster angle when polarized light is reflected at a dielectric-conductor interface," J. Opt. Soc. Am. A **25**, 2858–2864 (2008).
31. R. M. A. Azzam and E. Ugbo, "Contours of constant pseudo-Brewster angle in the complex ε plane and an analytical method for the determination of optical constants," Appl. Opt. **28**, 5222–5228 (1989).